Identification and Characterization of Circular RNAs in Brassica rapa in Response to Plasmodiophora brassicae

Huishan Liu
Shenyang Agricultural University
Chinedu Charles Nwafor
Nebraska-Lincoln
Yinglan Piao
Shenyang Agricultural University
Xiaonan Li
Shenyang Agricultural University
Zongxiang Zhan
Shenyang Agricultural University
Zhongyun Piao (zypiao@syau.edu.cn)
Shenyang Agricultural University

Research Article

Keywords: clubroot, disease resistance, Brassica rapa, circRNAs, Plasmodiophora brassicae

Posted Date: August 20th, 2021

DOI: https://doi.org/10.21203/rs.3.rs-666198/v1

Abstract

Background

Plasmodiophora brassicae is a soil-borne pathogen that attacks the roots of cruciferous plants, causing clubroot disease. CircRNAs are non-coding RNAs widely exist in plant and animal species which can acting as “microRNA (miRNA) sponges” and “competing endogenous RNAs (ceRNAs)”. Knowledge of circRNAs has been updated continuously and rapidly. However, the information about circRNAs in the regulation of clubroot-disease resistance is limited in *Brassica rapa*.

Results

Here, the Chinese cabbage (BJN 222) containing clubroot resistance gene (*CRa*) resistant to the Pb4 was susceptible to the PbE of *P. brassicae*. To investigate the mechanism of cicRNAs responsible for clubroot-disease resistance in *Brassica rapa*, the circRNA-seq was performed roots of BJN 222 at 0 d, 8 d, and 23 d after inoculated with Pb4 and PbE. A total of 1636 circRNAs were detected distributed on 10 chromosomes. Furthermore, total 231 differentially expressed circRNAs between groups were screened. Parental genes of circRNAs functions analysis results indicated that the expression of circRNAs was affected not only by inoculation time but also by the pathogenicity of *P. brassicae.* However, the “Phenylalanine, tyrosine, and tryptophan biosynthesis” pathway was significant enriched between the two pathotypes at different inoculation times. All the expression of target genes annotated with “receptor-like protein kinase,” “zinc finger protein,” “LRR-repeat protein,” and “hormone-related” identified from the circRNA-miRNA-mRNA network were analyzed. 5 target genes were consistent with the expression pattern of *novel_circ_000495* at 8 dpi, but only *Bra026508* was significantly up-regulated.

Conclusion

The up-regulated *novel_circ_000495* might suppressed the expression of *miR5656-y*, leading to the up-regulation of *Bra026508*. Our results provided new insights to clubroot resistance mechanisms of *B.rapa* and laid a foundation for further research on the function of circRNAs responsible for the pathogen infection.

Background

Eukaryotic cells contain two main type of ribonucleic acids (RNAs): messenger RNAs (mRNAs) and non-coding RNAs (ncRNAs). mRNAs and ncRNAs are generated by genomic transcription, but ncRNAs are not translated into proteins, including microRNAs (miRNAs), circular RNAs (circRNAs), and long-non coding RNAs (lncRNAs). Non-codind RNAs have emerged as important molecules for the transcriptional and post-transcriptional regulation of gene expression in plants, and an increasing body of evidence show their extensive function including interaction with mRNA under different conditions in plant development, biotic and abiotic stress responses (Ariel et al., 2015; Wang et al., 2017a).

Previously, circRNAs were identified as non-functional byproducts of genomic transcription in hunams (Hsu and Coca-Prados, 1979; Sanger et al., 1976), however resent studies suggest are wide spread in eukaryotes and play an important role in life activities of organisms (Qu et al., 2015). Circular RNAs (circRNAs) are new endogenous non-coding RNAs produced from precursor messenger RNAs characterized by a covalent bond connecting the 3’ and 5’ ends processed from back splicing (Jeck et al., 2013; Ashwal-Fluss et al., 2014). CircRNAs can be classified into exon circRNAs, intronic circRNAs, exon-intron circRNAs, intergenic circRNAs, and antisense circRNAs based

on their source. The proportions of these types of circRNA vary among different species. In *rice* and *Arabidopsis,* the exon circRNAs accounted for the greater portion of circRNAs, intergenic circRNAs are the highest proportion of circRNAs found in *kiwi*, *wheat*, *soybean*, and *potato*, and *tomato* (Lu et al., 2015; Chen et al., 2017; Wang et al., 2017b; Zhao et al., 2017; Zhou et al., 2018). Similar to microRNA (miRNA) and long non-coding RNA (lncRNA), circRNA is gaining much attention in the field of non-coding RNAs (Qu et al., 2015). An increasing body of evidence suggests that circRNAs play important roles in regulating the function of microRNAs (miRNAs), splicing and transcription, including the modification of gene expression, indicating that circRNAs might have essential functions in plant growth and development of (Li et al., 2018).

Earlier reports of function of circRNA with animal systems have implicated circRNA in the regulation of human disease condition (Burd et al., 2010; Memczak et al., 2013; Salzman et al., 2013; Li et al., 2015). Compared with the advances of circRNAs in animals, the knowledge of circRNAs in plants is limited. In recent years, it has been reported that circRNAs express in a wide range of eukaryotic species, including *Arabidopsis thaliana*, *rice*, *tomato*, *maize*, and Chinese cabbage (Chen et al., 2017; Wang et al., 2019; Zhou et al., 2019; Fan et al., 2020). Also, there are reports showing that circRNAs function plays a role in fiber development, flowering, and fruit coloration (Tan et al., 2017; Tong et al., 2018).

Recent reports suggest abiotic and biotic stress affect the abundance and expression of circRNAs, including pathogen invasion (Zhao et al., 2017; Ghorbani et al., 2018; Gao et al., 2019). Zhou et al. have shown that the expression of circRNAs changes considerably under abiotic stress. Under high-temperature stress, 73 out of 748 circRNAs were significantly expressed in tomato seeds than control (Zhou et al., 2019). Under chilling stress, 163 circRNAs exhibit chilling responsive expression in tomato (Zuo et al., 2016), which supports their role as novel interactors in regulating gene expression in plants. Darbani et al. reported that circRNAs regulate genes that are involved in several aspects of cellular metabolism as hormonal signaling, intracellular protein sorting, carbohydrate metabolism, and cell-wall biogenesis, respiration, amino acid biosynthesis, transcription and translation, and protein ubiquitination (Darbani et al., 2016). In *Arabidopsis*, the overexpressing circGORK (Guard cell outward-rectifying K+ -channel) resulted in hypersensitive to abscisic acid, but insensitive to drought suggesting a positive role of circGORK in drought tolerance (Zhang et al., 2019). Meanwhile, CircRNAs show differential expression due to biotic stressors. For example, 584 circRNAs were founded differentially expressed in *kiwifruit* after canker pathogen infection (Wang et al., 2017d). Also, a recent study confirmed that differential expression circRNAs might play roles during the *potato-Pectobacterium carotovorum subsp. Brasiliense* (Pcb) interaction (Zhou et al., 2017). A total of 280 differentially expressed circRNAs were found in cotton infected with Verticillium wilt. The number of differentially expressed circRNAs in the susceptible line was approximately twice as many circRNAs as disease-resistant line, and the differential expression levels of the circRNAs were generally higher in disease-resistant line than in the susceptible line (Xiang et al., 2018). Wang et al. (2018) showed 32 and 83 specific expressions of circRNAs between *tomato* leaves infected with YLCV (yellow leaf curl virus) and the control, respectively, and the expression level of circRNAs after infection with the virus was lower than that of the control. Together, these results indicated that circRNAs responds to biological stress and may participate in the regulation of plant development.

Clubroot, caused by the soil-borne obligate intracellular parasite *Plasmodiophora brassicae*, is a severe and worldwide disease of the *Brassicaceae* (Liu et al., 2018). The severe root damage caused by *P. brassicae* dramatically restricts water and nutrient transport from the roots resulting in stunted plants and tremendous yield loss. However, some cruciferous plants have acquired a certain degree of defense mechanisms during evolution,

including resistant genes, Secondary metabolites, cell wall modifications and plant hormone signaling pathways in response to *P. brassicae* (Robert-Seilaniantz et al., 2011). Recently, it has been reported that lncRNAs and miRNA participate in resistance to this disease. However, role of circRNAs in the onset of the disease has not been studied.

Moreover, research into the relationship between circRNAs and clubroot disease is rare. In this study, we aim identify and characterize the circRNAs involved in clubroot disease conditioning in *Brassica rapa.* Here we infected the Chinese cabbage (BJN 222) with two types of P*. brassicae* pathotype and identified and analyzed circRNAs from three stages (0 dpi, 8 dpi, 23 dpi). We detected more than one thousand circRNAs, among which over two hundred were differentially expressed, suggesting that circRNAs were effective indicators of plant resistance. In addition, the differentially expressed circRNAs were identified, and their parental functional annotations were analyzed. Moreover, circRNA-originating target miRNA predictions were made to predict the function of circRNAs in *Brassica rapa*. Our study will provide an essential resource for future circRNAs analysis in plant resistance of *Brassica rapa*.

Materials And Methods

Plant materials and inoculation with *P. brassicae*

Chinese cabbage “BJN 222” harboring the *CRa* resistant gene was resistant to the pathotype 4 (Pb4) but susceptible to the pathotype E (PbE) of *P.brassicae*, which was confirmed in the inoculation experiment. The *CRa* gene of “BJN 222” was derived from resistant material CR Shinki DH line (Piao et al. 2002). The seeds of these two resistant materials were kept in College of Horticulture, Shenyang Agriculture University, Shenyang City, Liaoning Province, China.

The Pb4 and PbE of *P. brassicae* were kept in College of Horticulture, Shenyang Agriculture University, Shenyang City, Liaoning Province, China. The Pb4 originated from Xinmin, Liaoning province, China (122°E, 41°N; China), and PbE originated from Shenyang, Liaoning province, China (123°E, 42°N; China). Both of them were maintained and propagated in the susceptible Chinese cabbage lines. For inoculation, 1 ml of Pb4 or PbE spore suspension (1.0×10^7 spores/mL) was applied to the stem base of 21-day-old Chinese cabbage plants. The inoculated and uninfected control plants were maintained in a climate-controlled room at 20℃-25℃ under a 16-h photoperiod. The soil was kept moist during the treatment period (Fu et al., 2019).

The roots of “BJN 222” were collected at 0, 8 and 23 days post-inoculation (dpi) to analyze genes that are differently expressed between plants infected with Pb4 compared with PbE. The roots of 30 plants were sampled at each time point, and three independent biological replicates (ten plants for each replicate) were performed. The roots were washed with distilled water and immediately frozen in liquid nitrogen and stored at -80℃. Ten plants of each replicate were pooled for further RNA extraction. To confirm the success of the infection, plants were maintained in the climate-controlled for 30 days after inoculation.

RNA and DNA isolation, library preparation and sequencing

According to the manufacturer's protocol, total RNAs from all samples (Table 1) above were extracted using TRIzol reagent (Invitrogen, Carlsbad, CA, USA). Total RNAs were treated with DNase I (Takara Bio, Dalian, China) to remove the contaminated genome DNA. The RNA purity of each sample was determined using a NanoDrop-

2000 spectrophotometer (Thermo Fisher Scientific, Wilmington, DE, USA). Samples with a 260/280 ratio of 1.9 - 2.1 and a 260/230 ratio ≥ 2.0 were considered to be of high quality and were used for experiments. And the RNA integrity was verified by 2.0% TAE agarose gel electrophoresis. For RNase R treatment, total RNAs were incubated for 15 - 30 min at 37 ℃ with 2 units RNase R per lμg of total RNA (Lucigen). RNA samples treated with or without RNase R were reverse transcribed with random primers using SuperScript II reverse transcriptase (Takara Bio, Dalian, China).

Table 1. The profile of sample information

Sample	treatment	replicate
0d-ck-1	control	biological replicate 1
0d-ck-2	control	biological replicate 2
0d-ck-3	control	biological replicate 3
8d-Pb4-1	inoculated with Pb4	biological replicate 1
8d-Pb4-2	inoculated with Pb4	biological replicate 2
8d-Pb4-3	inoculated with Pb4	biological replicate 3
8d-PbE-1	inoculated with PbE	biological replicate 1
8d-PbE-2	inoculated with PbE	biological replicate 2
8d-PbE-3	inoculated with PbE	biological replicate 3
23d-Pb4-1	inoculated with Pb4	biological replicate 1
23d-Pb4-2	inoculated with Pb4	biological replicate 2
23d-Pb4-3	inoculated with Pb4	biological replicate 3
23d-PbE-1	inoculated with PbE	biological replicate 1
23d-PbE-2	inoculated with PbE	biological replicate 2
23d-PbE-3	inoculated with PbE	biological replicate 3

Mapping to the reference genome and transcriptome assembly

20 mers from both ends of the unmapped reads were extracted and aligned to the reference genome (Version 1.5, http://brassicadb.org/brad/datasets/pub/Genomes/Brassica_rapa/V1.0/V1.5) to find unique anchor positions within the splice site. Anchor reads aligned in the reversed orientation (head-to-tail) indicated circRNA splicing and then were subjected to find_circ (Lv et al., 2020) to identify circRNAs. The anchor alignments were then extended such that the complete read aligns and GU/AG splice sites flanked the breakpoints. A candidate circRNA was called if supported by at least two unique back spliced reads at least in one sample.

To identify differentially expressed circRNAs across samples or groups, the edgeR package (http://www.rproject.org/) was used. The RPM (reads per million mappings) was used to evoluate the relative expression levels of the circRNAs. The expression levels of the circRNAs in the three replications were averaged as

the final result for one treatment. Significantly differentially expressed circRNAs were identified by the paired t-test with $P < 0.05$ and $|\log_2 FC|$ (fold change/FC) > 1 between samples or groups.

CircRNA detection and functional annotation

To evaluate the potential functions of parental genes of circRNAs, the parental genes were annotated base on the GO (Gene Ontology) database and KEGG (Kyoto Encyclopedia of Genes and Genomes) database. According to gene ontology (GO) annotation, the genes were functionally categorized by using BLAST2GO software (Conesa et al., 2005). The GO database includes three ontologies: molecular function, cellular component, and biological process. Pathway enrichment analysis identified significantly enriched metabolic pathways or signal transduction pathways in parental genes compared with the whole genome background. Pathways meeting the condition of p 0.05 were defined as significantly enriched pathways in parental genes.

CircRNA miRNA-binding sites analysis

For circRNAs that have been annotated in circBase, the target relationship with miRNAs can be predicted by StarBase (v2.0). For novel circRNAs, the software postmatch (v1.2) was used to predict target genes for plant samples.

Integrated analysis of circRNAs-miRNAs-mRNAs

For predicting mRNAs interacting with circRNAs and miRNAs, miRTarBase (v6.1) was used to predict mRNAs targeted by miRNAs sponge. Cytoscape can visualize the resulting correlation of circRNAs-miRNAs-mRNAs.

CircRNA validation and Quantitative Real-Time PCR

Primers (convergent and divergent) were designed using the Primer5.0 software. Furthermore, the primers were further synthesized by Synbio Tech (Suzhou, China). Both genomic DNA (gDNA) and cDNA (RNase R+ or RNase R-) were used as the template for the convergent and divergent primers. Real-time Quantitative Polymerase Chain Reaction (qRT-PCR) was performed to validate the expression of circRNAs. The qPCR was carried out in a total volume of 20 μL contained 10 μL of SYBR Premix ExTaq (2×), 0.5 μL of each primers (10 μM), 2 μL diluted cDNA, and 7 μL ddH_2O (TIANGEN). Each sample was amplified with three technical replicates and all PCR reactions were performed with BIORAD CFX96 Real-Time System PCR. The qPT-PCR program was as follows: 95 ℃ for 15 min, followed by 40 cycles of 95 ℃ for 10 s, 60 ℃ for 25 s, and 72 ℃ for 30 s. The specificity of amplification was confirmed by melting curve analysis after 40 cycles. Analysis of gene expression was performed for all samples at 0, 8, 23 dpi of “BJN 222” inoculated with Pb4 and PbE. The $2^{-\Delta\Delta CT}$ method was using to relative calculated the expression of circRNAs (Livak et al., 2001)

Results

The RNA-seq of circRNAs in *B. rapa*

Total 15 RNA-seq libraries (five samples, ck-0d, Pb4-8d, Pb4-23d, PbE-8d, PbE-23d, with three biological replicate, SUB9677054) were constructed and sequenced. A total of 2.07×10^{11} raw reads were obtained. After removing low-quality reads, adaptor reads, and rRNA reads, a total of 1.3 billion clean reads were generated and mapped to

B. rapa reference genome. The ratios of uniquely mapped reads range from 58.73 % to 77.91 % (Table 2) and only high-quality clean reads were used further circRNA analysis.

Table 2. Detailed information of sequenced data for each sample

Sample	Total Reads	Unmapped Reads	Unique Mapped Reads	Multiple Mapped reads	Mapping Ratio
ck-0d-1	94830544	20944005 (22.09%)	73261939 (77.26%)	624600 (0.66%)	77.91%
ck-0d-2	83307918	19608143 (23.54%)	63175699 (75.83%)	524076 (0.63%)	76.46%
ck-0d-3	87178800	21098697 (24.20%)	65551669 (75.19%)	528434 (0.61%)	75.8%
Pb4-8d-1	79369378	18691738 (23.55%)	60148368 (75.78%)	529272 (0.67%)	76.45%
Pb4-8d-2	87104958	29049743 (33.35%)	57582187 (66.11%)	473028 (0.54%)	66.65%
Pb4-8d-3	91092828	25243306 (27.71%)	65297978 (71.68%)	551544 (0.61%)	72.29%
PbE-8d-1	92293366	25751295 (27.90%)	65994329 (71.50%)	547742 (0.59%)	72.1%
PbE-8d-2	90149442	24266260 (26.92%)	65323398 (72.46%)	559784 (0.62%)	73.08%
PbE-8d-3	95240094	24798804 (26.04%)	69841392 (73.33%)	599898 (0.63%)	73.96%
Pb4-23d-1	73820444	25455609 (34.48%)	48002827 (65.03%)	362008 (0.49%)	65.52%
Pb4-23d-2	86986186	35568332 (40.89%)	51024370 (58.66%)	393484 (0.45%)	59.11%
Pb4-23d-3	90911480	34229301 (37.65%)	56256863 (61.88%)	425316 (0.47%)	62.35%
PbE-23d-1	96886026	35891103 (37.04%)	60538395 (62.48%)	456528 (0.47%)	62.96%
PbE-23d-2	88712612	35756006 (40.31%)	52569290 (59.26%)	387316 (0.44%)	59.69%
PbE-23d-3	105084474	43371402 (41.27%)	61241798 (58.28%)	471274 (0.45%)	58.73%

Identification and validation of circRNAs

Total 1636 novel circRNAs were detected from our circRNA-seq data and named from *novel_circ_000001* to *novel_circ_001636* after BLAST searches against the circBase database (Glažar er al., 2014; Xiang et al., 2018; Lv et al., 2020).

According to the genome origination, the 1636 circRNAs were classified into six types, including annot_exons, one_exon, intronic, exon_intron, intergenic, and antisense, containing 100, 342, 13, 408, 201, and 572 circRNAs, respectively (Figure 1A). The number of circRNAs encoded by antisense and intronic regions accounting for the most and the least (34.9% and 0.7%), respectively. The annot_exons, one_exon, and exon_intron-type circRNAs containing the exon sequence account for most of the 1636 circRNAs (approximately 51.96%). These results are consistent with the studies in other species, such as *Arabidopsis thaliana* and *Oryza sativa*, whose circRNAs originated from exons of a single protein-coding gene, accounting for 50.5% and 85.7%, respectively (Ye et al., 2015). The distribution of these circRNAs on the chromosome of *B.rapa* ranged from 81 to 255 (Figure 1B). For example, 255 circRNAs from chromosome A06 accounted for the most (15.59%), followed by chromosome A01 and chromosome A09. The length distribution of these circRNAs ranged from 101 to 2,000 bp. Furthermore, the largest number of circRNAs was the length ranged from 201 to 300 bp (Figure 1C).

To validate the circular RNAs detected from RNA sequencing, several circRNA were randomly selected for polymerase chain reaction amplification. A pair of convergent primers were designed to amplify the linear DNA fragments when cDNA or genomic DNA was used as templates in the PCR reactions. Unlike convergent primers, the reverse primers of the divergent primers were located upstream of the forward primers (Figure 2A). The amplification products were not detected in genomic DNA samples with divergent primers (Figure 2B, the original gel image is shown in additional file 1). On the contrary, there were no amplification products in the cDNA digested by RnaseR with convergent primers. After confirmation by PCR reaction, sequencing analyses were used to confirm the junction sites of PCR products (Figure 2C). In total, 30 circRNAs were validated by PCR reactions. 28 of the 30 circRNAs (93.3%) were validated in our experiments. Next, we randomly selected 15 circRNAs at a different stage for qRT-PCR to validate the expressing levels. The qRT-PCR results mainly were (12/15) consistent with the RNA-seq data, indicating the high reliability of the RNA profiles (Figure 3, Additional file 2).

Diagram of circular RNA junction site. Arrow direction indicates the direction of divergent primer design. (B)The PCR reactions with divergent and convergent primers using different templates showing the production of novel-circ-001061. (C)Sequencing confirmation of the junction site of novel-circ-001061.

CircRNAs analysis in response to *P. brassicae*

To explore the expression pattern of circRNA in response to the different pathotypes of *P.brassicae in B.rapa*, circRNA expression profiles of all the samples were compared by cluster analysis. The expression pattern of circRNA as divided into two different clusters based on infection time (Figure 4). At the later stage of inoculation, the circRNA response to two pathotypes of *P.brassicae* showed obviously differences. Although in the same cluster, there was significant difference between uninoculated samples and 8-days post inoculation samples, regardless of the pathotypes suggesting that the circRNA pattern of expression was affected by the inoculation time and pathotype of *P.brassicae* (Additional file 3). A total of 231 significantly differentially expressed circRNAs between the 8 comparisons were detected. There was no significant difference in the number of up/down-regulated circRNAs between the samples inoculated with PbE or Pb4 at 8 dpi (24 versus 27). With the inoculation time increasing, the number of DE circRNAs increased up to 118 in the samples inoculated with PbE, 76 circRNAs were up-regulated, and 42 circRNAs were down-regulated (Figure 4). However, the number of DE circRANs were only 64 inoculated with Pb4 at 23 dpi. The difference in the number of DE circRNAs implied that *B. rapa* was sensitive to the infection by virulent *P. brassicae* pathotype. Overall, the number of differentially expressed

circRNAs infected with PbE was greater than that of circRNAs infected with Pb4. These results highlight the distinct responses of “BJN 222” to pathogens exhibiting varying degrees of virulence.

Figure 5, shows the result of data-set overlap, here compared with ck, specifically DE circRNAs were 18 and 15 in Pb4 and PbE at the time of 8 dpi, respectively. Furthermore, identified 22 and 76 specifically DE circRNAs at 23 dpi in samples inoculated with Pb4 and PbE, respectively (Figure 5). In addition, 25 circRNAs were co-expressed after inoculated with Pb4 or PbE at the comparison of 8 dpi and 23 dpi. And only 1 circRNA was find continuously expressed after inoculation with PbE at the two-time point (Figure 5). Whether inoculated with Pb4 or PbE, the number of specifically DE circRNAs at 23 dpi is much larger than that at 8 dpi, suggesting that *B.rapa* responded differently to a different inoculation time. The specifically expressed circRNAs in plants inoculated with PbE were 4 fold than that of Pb4 at 23dpi, suggesting that *B.rapa* responded differently to different *P. brassicae* pathotype. Together, these results suggest that circRNAs participate in transcriptome-wide molecular landscapes of *B. rapa* responses to the *P. brassicae* stress.

Identification of circRNA parental genes

The annotated genes producing circRNAs are referred to as the parental genes of the circRNAs, while the circRNAs without parental genes were described as ‘NA’. Here a total of 1435 of the identified 1636 circRNAs originated from 1004 parental genes, and 201 intergenic-type circRNAs originated from the fragment between two genes without parental genes (Additional file 4). A total of 826 circRNAs have only one parental gene, and 609 circRNA originated from more than one parental gene. The parental genes produced different circRNAs due to the alternative splicing pattern in *B.rapa*, which is consistent with previous studies that suggest circRNAs possess an alternative splicing pattern, making it a valuable resource for understanding the complexity of circRNA biogenesis and their potential functions of circRNAs (Zhang et al., 2016; Gao et al., 2016).

CircRNA parental genes functions analysis

The circRNAs play significant roles in transcriptional control by cis-regulation of their host genes (Li et al., 2015). In order to gain insight into the potential circRNAs mediated mechanism of *B.rapa* response to the infection of *P. brassicae*, the KEGG pathway enrichment analysis method was employed to analyze the DE circRNA parental genes. The comparison between avirulent Pb4 and control group at 8 dpi showed that the DEGs were enriched in “Sulfur metabolism” (ko00920), “Microbial metabolism in diverse environments” (ko01120), “Citrate cycle (TCA cycle)” (ko00020) (p□0.05) (Figure 6A, Additional file 5). However, no significant pathway enrichment was detected at 23dpi between the two groups. We also compared the virulent PbE and control group at 8 dpi, and one significant pathway enrichment was detected i.e., “Sulfur metabolism” (ko00920) (p□0.05), while the pathway “Vitamin B6 metabolism” (ko00750) were enriched at 23 dpi (Figure 6C, Figure 6D, Table S2). The pathway like “Phenylalanine, tyrosine and tryptophan biosynthesis” (ko00400) was significantly enriched in the comparison of PbE vs. Pb4 at 8 dpi and 23 dpi (Figure 6E, Figure 6F). Tryptophan biosynthesis was involved in SA and camalexin biosynthesis. The plant hormone salicylic acid (SA) plays a critical role in defense against biothrophic pathogens such as *Plasmodiophora brassicae* (Miao et al., 2019); and camalexin is a sulfur-containing tryptophan-derived secondary metabolite, reported to play defensive functions against several pathogens in Arabidopsis (Ausubel et al., 1995; Glawischnig, 2007).

GO (Gene Ontology) analysis was performed on the parental genes to understand the biological function of the DE circRNAs. The parental genes were classified into three GO categories: biological process, molecular function,

and cellular component. The top five subcategories in the biological processes class such as “cellular process”, “single-organism process”, “metabolic process”, “response to stimulus”, and “localization” were enriched (Additional file 6, Additional file 7), implying that the parental genes of circRNAs may function in response to the infection of *P.brassicae*. The most highly represented molecular function categories were “catalytic activity” and “binding”. The top 3 subcategories in the cellular component class, were “cell”, “cell part”, and “organelle”. Similarly KEGG pathway enrichment analysis results, “metabolic process” and “response to stimulus” were overrepresented at every in all the comparison groups, and the number of DEGs was significantly higher at 23 dpi than 8 dpi.

Together, many parental genes responded to rhizobium stress. Also, the amount of DE circRNA varied considerably over time, but there were most pathways of enrichment associated with metabolic processes, which may be due to plant life activities rather than stimulation of *P. brassicae*. Therefore, we focus on the circRNAs and related genes of significant enrichment pathways at the early stage infected with *P. brassicae* (Table 3). Furthermore, the parental genes and their annotations in each comparison was shown as Additional file 8. By predicting the function of parental genes, the circRNAs origined from *Bra012389* and *Bra019293* were selected for further study.

Table 3. The circRNAs and their parental genes in each comparison

Group	CircRNA ID	Soure gene ID	log2(FC)	P value	chr	strand	Type
ck-0d-vs-Pb4-8d	novel_circ_000064	Bra013579*	4.246827502	0.004744418	A01	-	exon_intron
	novel_circ_000079	Bra013579*	2.893516888	0.009588829	A01	-	exon_intron
	novel_circ_000086	Bra013579*	-2.84065774	0.028360819	A01	+	antisense
	novel_circ_000264	Bra039746*	-19.12803312	0.04701868	A02	+	exon_intron
ck-0d-vs-PbE-8d	novel_circ_000074	Bra013579*	19.51979677	0.011219066	A01	-	exon_intron
	novel_circ_000086	Bra013579*	-3.947713015	0.012980797	A01	+	antisense
PbE-8d-vs-Pb4-8d	novel_circ_001061	Bra012389*	-4.222569626	0.038710775	A07	-	exon_intron
	novel_circ_000495	Bra019293*	4.995712702	0.001038162	A03	-	antisense

Note: *indicate that it is a significant difference at 0.05 level.

CircRNAs acting as miRNA sponges

To determine whether circRNAs in *B.rapa* could affect post-transcriptional regulation by binding to miRNAs and preventing them from regulating their target mRNAs, we identified miRNA target sites of circRNAs in *B.rapa*, and found that 257 of 1636 (15.7%) circRNAs had putative miRNA-binding sites (Additional file 9). Of this 257 circRNAs, 116 had more than one different miRNA-binding site, and the greatest number of miRNA-binding sites (39) was found in *novel_circ_000502*. Like *novel_circ_000769* only had one miRNA-binding site, and *novel_circ_001061* and *novel_circ_000495* had 2, 3 miRNA-binding sites, respectively (Figure 7). The *miR5021-x* and *miR2275-x* account for most of the circRNAs (55, 38, respectively). These results indicated that circRNAs in

B.rapa have many potential miRNA binding sites and probably affected the expression of disease-resistant genes through miRNA.

Schema diagrams show the pairing of each circRNA sequence and the sequence of its target region.

Construction of circRNA-miRNA-mRNA network

To better understand the gene regulatory network during the infection of *Brassica rapa*, the DE circRNAs and their parental genes in the PbE-8d-vs-Pb4-8d group were selected for the circRNA-miRNA-mRNA network analysis with Cytoscape software (Additional file 10, Additional file 11) (Liang et al., 2019). By predicting the miRNAs and their target genes of circRNAs, many miRNA-targeted mRNAs were annotated to be stress-associated. 20 target genes were annotated with “receptor-like protein kinase”, “zinc finger protein”, “LRR-repeat protein” and “hormone-related” functions (Additional file 12). The relative expression level of these candidate target genes showed diverse expression patterns (Figure 8). Here, 5 target genes, *Bra011339* (zinc finger protein), *Bra013568* (zinc finger protein), *Bra026508* (hormone-related), *Bra036269* (LRR-repeat protein) were consistent with the expression pattern of *novel_circ_000495* at 8 dpi (Figure 9A). However, only *Bra026508* showed significantly different expression between the inoculation of Pb4 and PbE (Figure 9B). Therefore, the circRNA *novel_circ_000495* probably plays an important role in clubroot resistance through post-transcriptional control of its target genes which are involved in biotic stress. Furthermore, more results are needed to confirm the function *Bra026508* in the *P. brassicae* resistance mechanism.

Discussion

CircRNA-Sequencing enriches understanding of mechanisms of clubroot resistance in *B.rapa*

In this study, the *B.rapa* disease-resistant variety “BJN 222” harboring the clubroot resistance gene (*CRa*) was inoculated with avirulent Pb4 or virulent PbE *P. brassicae*; transcriptome sequencing revealed a large number of differentially expressed circRNAs at 0, 8, and 23 dpi. Here, 1636 novel circRNAs were identified during *P. brassicae*-*B.rapa* interaction, and the contributions of the five group of *B.rapa* to the generated circRNAs was approximately the same, indicating that circRNAs are universally present in *Brassica rapa*. Our results suggest that significant changes occurred in the transcriptome of *B. rapa* during infection with the two types of the pathogen, especially in the expression levels of many genes that we detected in the different disease condition. For example the number of differentially expressed circRNAs at 23 dpi is significantly higher than that of 8 dpi, which is consistent with Fu Pengyu et al. Additionally, the number of differentially expressed circRNAs in PbE at 23 dpi was significantly higher than that of Pb4 (118 to 64), indicating that Chinese cabbage had different responses to various degrees of *P.brassicae* infection. Whether these differentially expressed circRNAs are related to the resistance of *P.brassicae* infection still needs to be verified by subsequent experiments.

Studies in rice have shown that multiple circRNAs can originate from a single gene (Lu et al., 2015), linked to alternative splicing (Zhang et al., 2016; Gao et al., 2016). In this study, multiple circRNAs from one parental gene also occurred, indicating that alternative back-splicing occurs in *B.rapa*. Gao et al. (2016) suggested that alternative splicing events in circRNAs are not always consistent with the corresponding mRNAs; therefore, the biogenesis, regulation, and function of alternatively spliced circRNAs in plants are worthy of further study.

Although circRNAs may not have the same function as the parental genes, some studies have shown that their functions are closely related. For example, circRNAs can interact with RNA polymerase II and promote transcription of their parental genes (Li et al., 2015); can reduce the expression of the source linear RNA (Tan et al., 2017); and promote the exon skipping of their parental genes (Conn et al., 2017). Therefore, most reports currently reflect the potential functions of circRNAs by studying the results of KEGG and GO function enrichment analysis of parental genes from which the circRNAs are derived (Pan et al., 2018; Zhou et al., 2018; Zeng et al., 2018). In the present study, pathway enrichment revealed that there are many small molecular compounds such as terpenoids, flavonoids, alkaloids,. that have been proven to be related to disease resistance (Guo et al., 2012). Such as tropane, piperidine, and pyridine alkaloid biosynthesis(ko00960), Ubiquinone and other terpenoid-quinone biosynthesis (ko00130), and the biosynthesis of amino acids (ko00400). In addition, the genes enriched in the Plant-pathogen interaction (Ko04626) pathway also have essential research significance. The result GO function analysis, revealed the proportion of differentially expressed genes in the 8 comparison groups. For example, molecular functions account for about 10.65%, biological processes account for about 54.74%, and cellular components account for about 34.61%. This is similar to the results of Chen et al. on the expression profile of soybean seeds at different developmental stages. Among the Biological Process GO terms such as “response to stimulus”, “immune system process” were significantly enrich and several of the genes that fell within this GO terms have been shown to be directly involved in disease resistance and stress response, implying that the circRNAs have participate in the responese of *P.brassicae.*

CircRNA acting as miRNA sponges affecting the function of target genes

CircRNAs can function as miRNA sponges, regulating the transcription of target genes (Qu et al., 2015). Such as *ciRS-7* (circular RNA sponge for *miR-7*), which was identified in human and mouse brain, has been found to have more than 70 conventional miRNA target sites and acts as a miRNA sponge regulating the function of *miR-7* (Hansen et al., 2013; Du et al., 2017). The mode of the action of miRNAs is different in plants and animals. Compared to plants the range of target genes regulated by miRNAs is relatively wide in animals. Many miRNAs can bind to partially complementary target gene regions to inhibit their translation process. In plants, the binding of miRNAs and target genes requires strict complementary base pairing (usually 2-4 base pair mismatches), and the target mRNA is directly degraded after binding. This relationship is often one-to-one. Reports suggest that miRNA-mediated cleavage may contribute to the degradation and low abundance of circRNAs in plants (Li et al., 2017). Until now, most studies on circRNAs have reported them as competing endogenous RNA (ceRNA) molecules for predictive analysis in plants (Liu et al., 2017; Zou et al., 2016; Wang et al., 2017b; Wang et al., 2017c). In this study founmultiple circRNAs differentially expressed under Rhizobium stress could target the same miRNA, and multiple miRNAs could target the same circRNA. Based on the results of KEGG and GO analysis, 2 significantly differentially expressed circRNAs were identified to have miRNAs (*miR7121-x*, *miR5656-y*, *miR3699-y*) binding sites, indicating that the circRNAs could interact with miRNAs to regulate gene expression in *B. rapa* which may be conserved in plants.

CeRNA networks could provide new sights into the regulatory roles of ncRNAs during the *P . brassicae* infection

Recently, the regulation of circRNAs, miRNAs, mRNAs have been confirmed in various diseases (Lin et al., 2018; Zhang et al., 2016). However, the circRNA-miRNA-mRNA regulatory network has not been widely constructed in plants.To uncover the ceRNA network and the functions of circRNAs during the *P. brassicae* infection in *B.rapa*, we constructed putative circRNA-miRNA-mRNA network. From the network, we could see that *novel_circ_000495* may

act as a miRNA sponge by targeting *miR5656-y* to regulate the expression of *Bra026508*, which function note was cytochrome P450 705A5-like. Cytochrome P450 is a heme-containing multifunctional oxidase that binds CO in its reduced state and has an absorption peak at 450 nm. P450s perform two types of biosynthetic and metabolic detoxification functions in plants, some of which have essential roles in plant defense responses. CYP705A5, encodes an endomembrane system-expressed member of the CYP705A family of cytochrome P450 enzymes. It appears to catalyze the addition of a double bond to thalian-diol at carbon 15. Reduced levels of THAD expression lead to a build-up of thalian-diol in root extracts. However, these mutants do not seem to have a higher susceptibility to Atlernaria brassicicola or Pseudomonas syringae pv. tomato DC3000 based on assays performed on seedling roots (Field et al., 2008). In the current study, it seems that the up-regulation of the *novel_circ_000495* suppressed the expression of *miR5656-y*, leading to the up-regulation of *Bra026508*. The up-regulated *Bra026508* might affect the plant resistance to different types of *P. brassicae* in *Brassica rapa*.

Abbreviations

B.rapa : *Brasscia rapa*

P. brassicae : *Plasmodiophora brassicae*

mRNA : messenger RNA

circRNA : Circular RNA

lncRNA : long non-coding RNA

miRNA : microRNA

ceRNA : competing endogenous RNA

Dpi : Days post-inoculation

FC : Fold change

RPM : Reads per million mappings

GO : Gene Ontology

KEGG : Kyoto Encyclopedia of Genes and Genomes

qRT-PCR : Real-time Quantitative Polymerase Chain Reaction

DEGs : Differentially expressed genes

Declarations

Ethics approval and consent to participate

This study does not include human or animal subjects.

Consent for publication

Not applicable.

Availability of data and material

The datasets analyzed during the current study are available in the SRA (BioProject ID PRJNA730971 , https://www.ncbi.nlm.nih.gov/bioproject/PRJNA730971) repository.

Competing interests

The authors all declare that they have no competing interests.

Funding

This study was supported by the National Natural Science Foundation of China (No. 31772326). Funds were used for the experimental conduction. The funders have no role in the design of the study and collection, analysis, and interpretation of data and in writing the manuscript.

Authors' contributions

Piao ZY, Zhan ZX, and Liu HS conceived and designed the experiments. Liu HS, Zhan ZX, Piao ZY, Piao YL, and Li XN analyzed the data. Liu HS analyzed the data, performed the experiments and drafted the manuscript. Zhan ZX, and Nwafor CC, helped to revise the manuscript. All the authors have read and approved the final manuscript.

Acknowledgments

We acknowledgment the time and expertise devoted to reviewing this manuscript by the reviewers and the members of the editorial board.

References

1. Ariel F, Romero-Barrios N, Jégu T, Benhamed M, Crespi M. Battles and hijacks: noncoding transcription in plants. *Trends Plant Sci.* 2015; 20(6):362-71. doi: 10.1016/j.tplants.2015.03.003.
2. Ashwal-Fluss R, Meyer M, Pamudurti NR, Ivanov A, Bartok O, Hanan M, et al. CircRNA biogenesis competes with pre-mRNA splicing. *Mol. Cell* 2014; 2;56(1):55-66. doi: 10.1016/j.molcel.2014.08.019.
3. Ausubel FM, Katagiri F, Mindrinos M, Glazebrook J. Use of *Arabidopsis thaliana* defense-related mutants to dissect the plant response to pathogens. *Proc. Natl. Acad. Sci. USA.* 1995; 9;92(10):4189-96. doi: 10.1073/pnas.92.10.4189.
4. Burd CE, Jeck WR, Liu Y, Sanoff HK, Wang Z, Sharpless NE. Expression of linear and novel circular forms of an INK4/ARF-associated non-coding RNA correlates with atherosclerosis risk. *PLoS Genet* 2010;2;6(12):e1001233. doi: 10.1371/journal.pgen.1001233.
5. Chen G, Cui J, Wang L, Zhu Y, Lu Z, Jin B. Genome-wide identification of circular RNAs in *Arabidopsis thaliana*. *Front. Plant Sci.* 2017; 27;8:1678. doi: 10.3389/fpls.2017.01678.
6. Conesa A, Götz S, García-Gómez JM, Terol J, Talón M, Robles M. Blast2GO: a universal tool for annotation, visualization and analysis in functional genomics research. *Bioinformatics* 2005; 15;21(18):3674-6. doi: 10.1093/bioinformatics/bti610.

7. Conn VM, Hugouvieux V, Nayak A, Conos SA, Capovilla G, Cildir G, et al. A circRNA from SEPALLATA3 regulates splicing of its cognate mRNA through R-loop formation. *Nat. Plants* 2017; 18;3:17053. doi: 10.1038/nplants.2017.53.
8. Darbani B, Noeparvar S, Borg, S. Identification of circular RNAs from the parental genes involved in multiple aspects of cellular metabolism in *Barley*. *Front. Plant Sci.* 2016); 3;7:776. doi: 10.3389/fpls.2016.00776.
9. Fan J, Quan W, Li GB, Hu XH, Wang Q, Wang H, et al. CircRNAs are involved in the *rice-magnaporthe oryzae* interaction. *Plant Physiol.* 2020; 182(1):272-286. doi: 10.1104/pp.19.00716.
10. Field B and Osbourn AE. Metabolic diversification-independent assembly of operon-like gene clusters in different plants. *Science* 2008; 320(5875):543-7. doi: 10.1126/science.1154990.
11. Fu PY, Piao ZY, Zhan ZX, Zhao YZ, Pang WX, Li XN. Transcriptome arofile of *Brassica rapa* L. reveals the involvement of jasmonic acid, ethylene, and brassinosteroid signaling pathways in clubroot resistance. *Agronomy* 2019; 9(10):589. doi: 10.3390/agronomy9100589
12. Gao Y, Wang J, Zheng Y, Zhang J, Chen S, Zhao F. Comprehensive identification of internal structure and alternative splicing events in circular RNAs. *Nat. Commun.* 2016; 7:12060. doi: 10.1038/ncomms12060.
13. Gao Z, Li J, Luo M, Li H, Chen Q, Wang L, et al. Characterization and cloning of *Grape* circular RNAs identified the cold resistance-related Vv-circATS1. *Plant Physiol.* 2019; 180(2):966-985. doi: 10.1104/pp.18.01331.
14. Ghorbani A, Izadpanah K, Peters JR, Dietzgen RG, Mitter N. Detection and profiling of circular RNAs in uninfected and *maize* Iranian mosaic virus-infected *maize. Plant Sci.* 2018; 274:402-409. doi: 10.1016/j.plantsci.2018.06.016.
15. Glawischnig E. Camalexin. *Phytochemistry* 2007; 68(4):401-6. doi: 10.1016/j.phytochem.2006.12.005.
16. Glažar P, Papavasileiou P, Rajewsky N. CircBase: a database for circular RNAs. *RNA* 2014; 20(11):1666–1670. doi:10.1261/rna.043687.113
17. Guo YL, Zhang PY, Guo MR, Chen KS. Secondary metabolites and plant defence against pathogenic disease. *Plant Physiol. J.* 2012; 48: 429–434. doi:10.13592/j.cnki.ppj.2012.05.010.
18. Hansen TB, Jensen TI, Clausen BH, Bramsen JB, Finsen B, Damgaard CK, et al. (2013). Natural RNA circles function as efficient microRNA sponges. *Nature* 495(7441):384-8. doi: 10.1038/nature11993.
19. Jeck WR, Sorrentino JA, Wang K, Slevin MK, Burd CE, Liu J, et al. Circular RNAs are abundant, conserved, and associated with ALU repeats. *RNA* 2013; 19(2):141-57. doi: 10.1261/rna.035667.112.
20. Li QF, Zhang YC, Chen YQ, Yu Y. Circular RNAs roll into the regulatory network of plants. *Biochem. Biophys. Res. Commun.* 2017;488(2):382-386. doi: 10.1016/j.bbrc.2017.05.061.
21. Li X, Yang L, Chen LL. The Biogenesis, Functions, and Challenges of Circular RNAs. *Mol. Cell* 2018; 71(3):428-442. doi: 10.1016/j.molcel.2018.06.034.
22. Li Y, Zheng Q, Bao C, Li S, Guo W, Zhao J, et al. Circular RNA is enriched and stable in exosomes: a promising biomarker for cancer diagnosis. *Cell Res.* 2015; 25(8):981-4. doi: 10.1038/cr.2015.82.
23. Li Z, Huang C, Bao C, Chen L, Lin M, Wang X, et al. Exon-intron circular RNAs regulate transcription in the nucleus. *Nat. Struct. Mol. Biol*. 2015; 22(3):256-64. doi: 10.1038/nsmb.2959.
24. Lin X and Chen Y. Identification of potentially functional circRNA-miRNA-mRNA regulatory network in hepatocellular carcinoma by integrated microarray analysis. *Med. Sci. Monit. Basic Res*. 2018; 24:70-78. doi: 10.12659/MSMBR.909737.

25. Liu T, Zhang L, Chen G, Shi T. Identifying and characterizing the circular RNAs during the lifespan of *Arabidopsis* leaves. *Front. Plant Sci.* 2017; 8:1278. doi: 10.3389/fpls.2017.01278.
26. Liu Y, Xu A, Liang F, Yao X, Wang Y, Liu X, et al. Screening of clubroot-resistant varieties and transfer of clubroot resistance genes to *Brassica napus* using distant hybridization. *Breed. Sci.* 2018; 68(2):258-267. doi: 10.1270/jsbbs.17125.
27. Livak KJ, Schmittgen TD. Analysis of relative gene expression data using real time quantitative PCR and the $2^{-\Delta\Delta CT}$ method. *Methods* 2001; 25(4):402–8. doi: 10.1006/meth.2001.1262.
28. Lu T, Cui L, Zhou Y, Zhu C, Fan D, Gong H, et al. Transcriptome-wide investigation of circular RNAs in rice. *RNA* 2015; 21(12):2076-87. doi: 10.1261/rna.052282.115.
29. Lv LL, Yu K, Lü HY, Zhang XQ, Liu XQ, Sun CY, et al. Transcriptome-wide identification of novel circular RNAs in soybean in response to low-phosphorus stress. *PLoS One* 2020; 21;15(1):e0227243. doi: 10.1371/journal.pone.0227243.
30. Memczak S, Jens M, Elefsinioti A, Torti F, Krueger J, Rybak A, et al. Circular RNAs are a large class of animal RNAs with regulatory potency. *Nature* 2013; 21;495(7441):333-8. doi: 10.1038/nature11928.
31. Miao Y, Xu L, He X, Zhang L, Shaban M, Zhang X, et al. Suppression of tryptophan synthase activates cotton immunity by triggering cell death via promoting SA synthesis. *Plant J.* 2019; 98(2):329-345. doi: 10.1111/tpj.14222.
32. Pan T, Sun X, Liu Y, Li H, Deng G, Lin H, et al. Heat stress alters genome-wide profiles of circular RNAs in *Arabidopsis*. *Plant Mol. Biol.* 2018; 96(3):217-229. doi: 10.1007/s11103-017-0684-7.
33. Piao ZY, Park YJ, Choi SR, Hong CP, Park JY, Choi YS, Lim YP. Conversion of AFLP marker linked to clubroot resistance gene into SCAR marker. *J Kor Soc Hortic Sci*. 2002;43:653– 659
34. Qu S, Yang X, Li X, Wang J, Gao Y, Shang R, et al. Circular RNA: A new star of noncoding RNAs. *Cancer Lett.* 2015; 365(2):141-8. doi: 10.1016/j.canlet.2015.06.003.
35. Robert-Seilaniantz A, Grant M, and Jones JD. Hormone crosstalk in plant disease and defense: more than just jasmonate-salicylate antagonism. *Annu. Rev. Phytopathol.* 2011; 49, 317–343. doi: 10.1146/annurev-phyto-073009-114447.
36. Salzman J, Chen RE, Olsen MN, Wang PL, Brown PO. Cell-type specific features of circular RNA expression. *PLoS Genet*. 2013;9(9):e1003777. doi: 10.1371/journal.pgen.1003777.
37. Sanger HL, Klotz G, Riesner D, Gross HJ, Kleinschmidt AK. Viroids are single-stranded covalently closed circular RNA molecules existing as highly base-paired rod-like structures. *Proc. Natl. Acad. Sci. USA.* 1976; 73(11):3852-6. doi: 10.1073/pnas.73.11.3852.
38. Tan J, Zhou Z, Niu Y, Sun X, Deng Z. Identification and functional characterization of *tomato* circRNAs derived from genes involved in fruit pigment accumulation. *Sci. Rep.* 2017; 7(1):8594. doi: 10.1038/s41598-017-08806-0.
39. Tong W, Yu J, Hou Y, Li F, Zhou Q, Wei C, et al. Circular RNA architecture and differentiation during leaf bud to young leaf development in tea (*Camellia sinensis)*. *Planta* 2018; 248(6):1417-1429. doi: 10.1007/s00425-018-2983-x.
40. Wang J, Meng X, Dobrovolskaya OB, Orlov YL, Chen M. Non-coding RNAs and their roles in stress response in plants. *Genomics Proteomics Bioinformatics* 2017a; 15(5):301-312. doi: 10.1016/j.gpb.2017.01.007.

41. Wang J, Yang Y, Jin L, Ling X, Liu T, Chen T, et al. Re-analysis of long non-coding RNAs and prediction of circRNAs reveal their novel roles in susceptible *tomato* following TYLCV infection. *BMC Plant Biol.* 2018; 18(1):104. doi: 10.1186/s12870-018-1332-3.
42. Wang W, Wang J, Wei Q, Li B, Zhong X, Hu T, et al. Transcriptome-wide identification and characterization of circular RNAs in leaves of Chinese cabbage (*Brassica rapa* L. *ssp. pekinensis*) in response to Calcium Deficiency-Induced Tip-burn. *Sci. Rep.* 2019; 9(1):14544. doi: 10.1038/s41598-019-51190-0.
43. Wang Y, Wang Q, Gao L, Zhu B, Luo Y, Deng Z, et al. Integrative analysis of circRNAs acting as ceRNAs involved in ethylene pathway in *tomato*. *Physiol. Plant* 2017b; 161(3):311-321. doi: 10.1111/ppl.12600.
44. Wang Y, Yang M, Wei S, Qin F, Zhao H, Suo B. Identification of circular RNAs and their targets in leaves of *Triticum aestivum* L. under dehydration stress. *Front. Plant Sci.* 2017c; 7:2024. doi: 10.3389/fpls.2016.02024.
45. Wang Z, Liu Y, Li D, Li L, Zhang Q, Wang S, et al. Identification of circular RNAs in *Kiwifruit* and their species-specific response to bacterial canker pathogen invasion. *Front. Plant Sci.* 2017d; 8:413. doi: 10.3389/fpls.2017.00413.
46. Du WW, Zhang C, Yang W, Yong T, Awan FM, Yang BB. Identifying and Characterizing circRNA-Protein Interaction. *Theranostics* 2017; 26;7(17):4183-4191. doi: 10.7150/thno.21299.
47. Xiang L, Cai C, Cheng J, Wang L, Wu C, Shi Y, et al. Identification of circular RNAs and their targets in *Gossypium* under Verticillium wilt stress based on RNA-seq. *PeerJ* 2018; 6:e4500. doi: 10.7717/peerj.4500.
48. Ye CY, Chen L, Liu C, Zhu QH, Fan L. Widespread noncoding circular RNAs in plants. *New Phytol.* 2015; 208(1):88-95. doi: 10.1111/nph.13585.
49. Zeng RF, Zhou JJ, Hu CG, Zhang JZ. Transcriptome-wide identification and functional prediction of novel and flowering-related circular RNAs from trifoliate orange (Poncirus trifoliata L. Raf.). *Planta* 2018; 247(5):1191-1202. doi: 10.1007/s00425-018-2857-2.
50. Zhang P, Fan Y, Sun X, Chen L, Terzaghi W, Bucher E, et al. A large-scale circular RNA profiling reveals universal molecular mechanisms responsive to drought stress in *maize* and *Arabidopsis*. *Plant J.* 2019; 98(4):697-713. doi: 10.1111/tpj.14267.
51. Zhang XO, Dong R, Zhang Y, Zhang JL, Luo Z, Zhang J, et al. Diverse alternative back-splicing and alternative splicing landscape of circular RNAs. *Genome Res.* 2016; 26(9):1277-87. doi: 10.1101/gr.202895.115.
52. Zhao W, Cheng Y, Zhang C, You Q, Shen X, Guo W, et al. Genome-wide identification and characterization of circular RNAs by high throughput sequencing in *soybean*. *Sci. Rep.* 2017; 7(1):5636. doi: 10.1038/s41598-017-05922-9.
53. Zheng Q, Bao C, Guo W, Li S, Chen J, Chen B, et al. Circular RNA profiling reveals an abundant circHIPK3 that regulates cell growth by sponging multiple miRNAs. *Nat. Commun.* 2016; 7:11215. doi: 10.1038/ncomms11215.
54. Zhou R, Yu XQ, Ottosen C, and Zhao TM. High throughput sequencing of circrnas in *tomato* leaves responding to multiple stresses of drought and heat. *Horticultural Plant Journal* 2018; 6(01):39-43. doi:10.1016/j.hpj.2019.12.004.
55. Zhou R, Yu XQ, Xu LP, Wang YL, Yu WG. Genome-wide identification of circular RNAs in *tomato* seeds in response to high temperature. *Biol. Plantarum* 2019; 63, 97–103.doi:10.32615/bp.2019.012
56. Zhou R, Zhu Y, Zhao J, Fang Z, Wang S, Yin J, et al. Transcriptome-wide identification and characterization of *potato* circular RNAs in response to rectobacterium carotovorum subspecies brasiliense infection. *Int. J. Mol.*

Sci. 2017; 19(1):71. doi: 10.3390/ijms19010071.

57. Zuo J, Wang Q, Zhu B, Luo Y, Gao L. Deciphering the roles of circRNAs on chilling injury in *tomato. Biochem. Biophys. Res. Commun.* 2016; 479(2):132-138. doi: 10.1016/j.bbrc.2016.07.032.

Figures

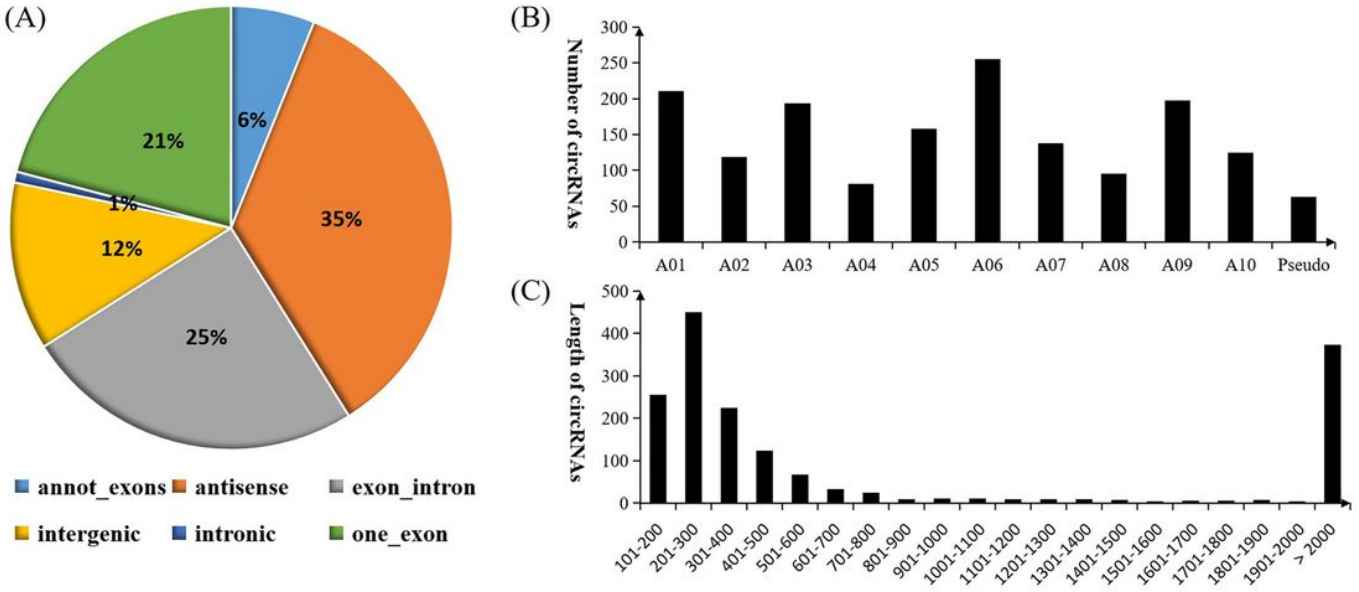

Figure 1

Characterization of circRNAs identified between control plants and plants infected with the two pathotypes of P.brassicae at 8 and 23 dpi. (A)Types of circRNAs. (B)Histogram of the distribution of circRNAs on the chromosome. (C)Distribution of the length of circRNAs.

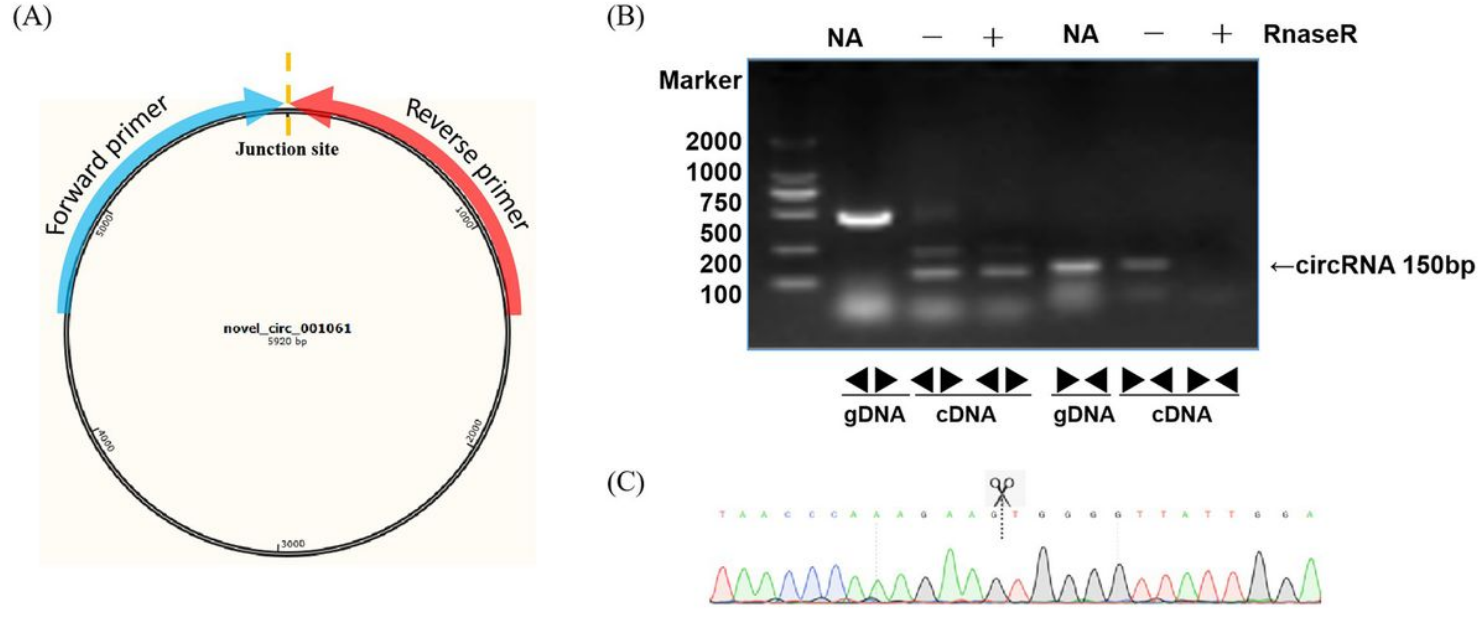

Figure 2

Validation examples of circRNA production. (A) Diagram of circular RNA junction site. Arrow direction indicates the direction of divergent primer design. (B)The PCR reactions with divergent and convergent primers using different templates showing the production of novel-circ-001061. (C)Sequencing confirmation of the junction site of novel-circ-001061.

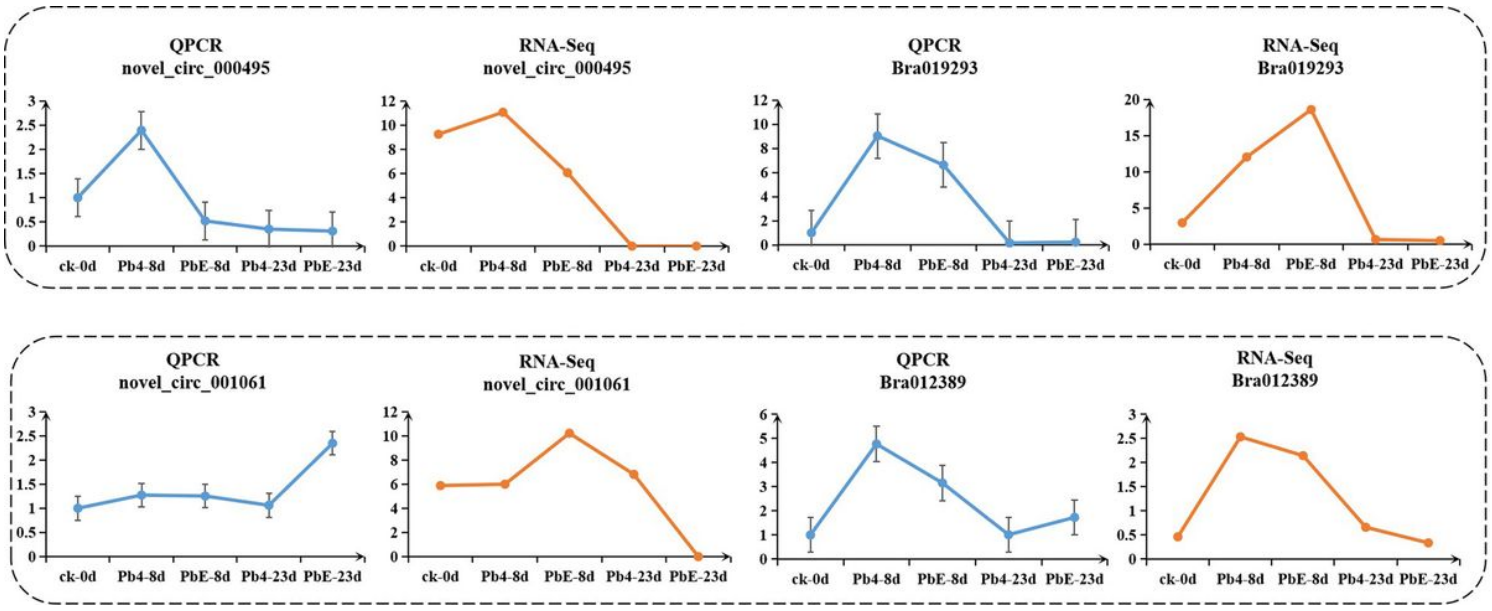

Figure 3

Quantitative real-time PCR validation for the RNA-seq data. (A) qRT-PCR validation of novel-circ-000495 and the parental gene. (B) qRT-PCR validation of novel-circ-001061 and the parental gene.

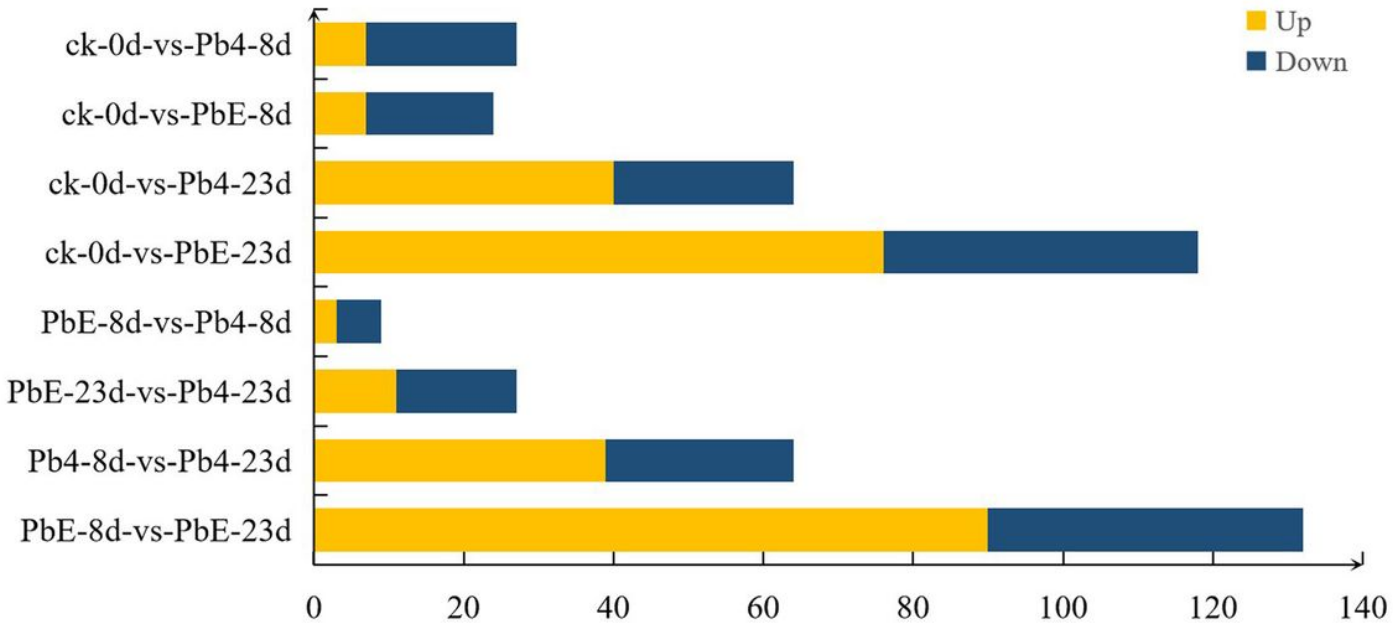

Figure 4

Comparison of the number of circRNAs between control plants and plants infected with the two pathotypes of P . brassicae at 8 and 23 dpi. Yellow and blue represent up-and down-regulated circRNAs, respectively. The results of 8 comparisons are shown.

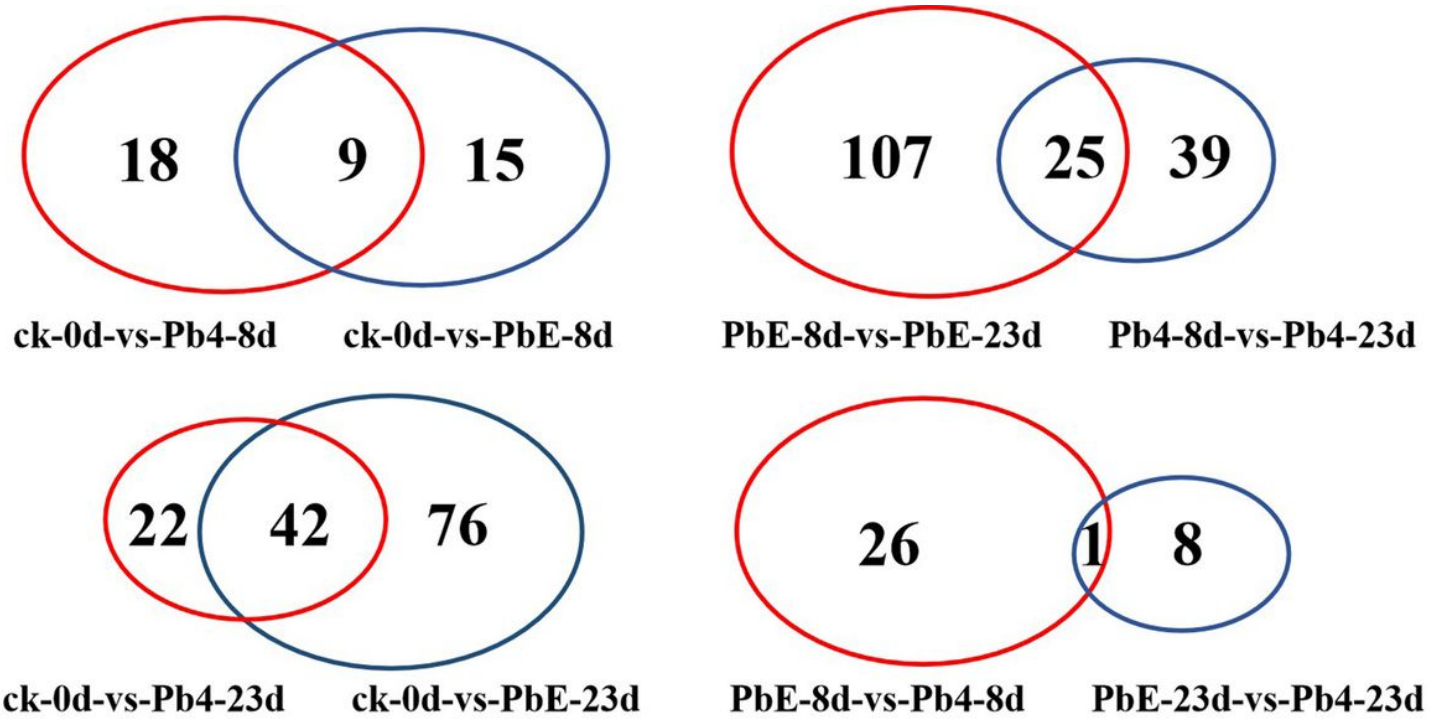

Figure 5

Venn diagrams showing the overlaps of circRNAs differentially expressed in each comparison.

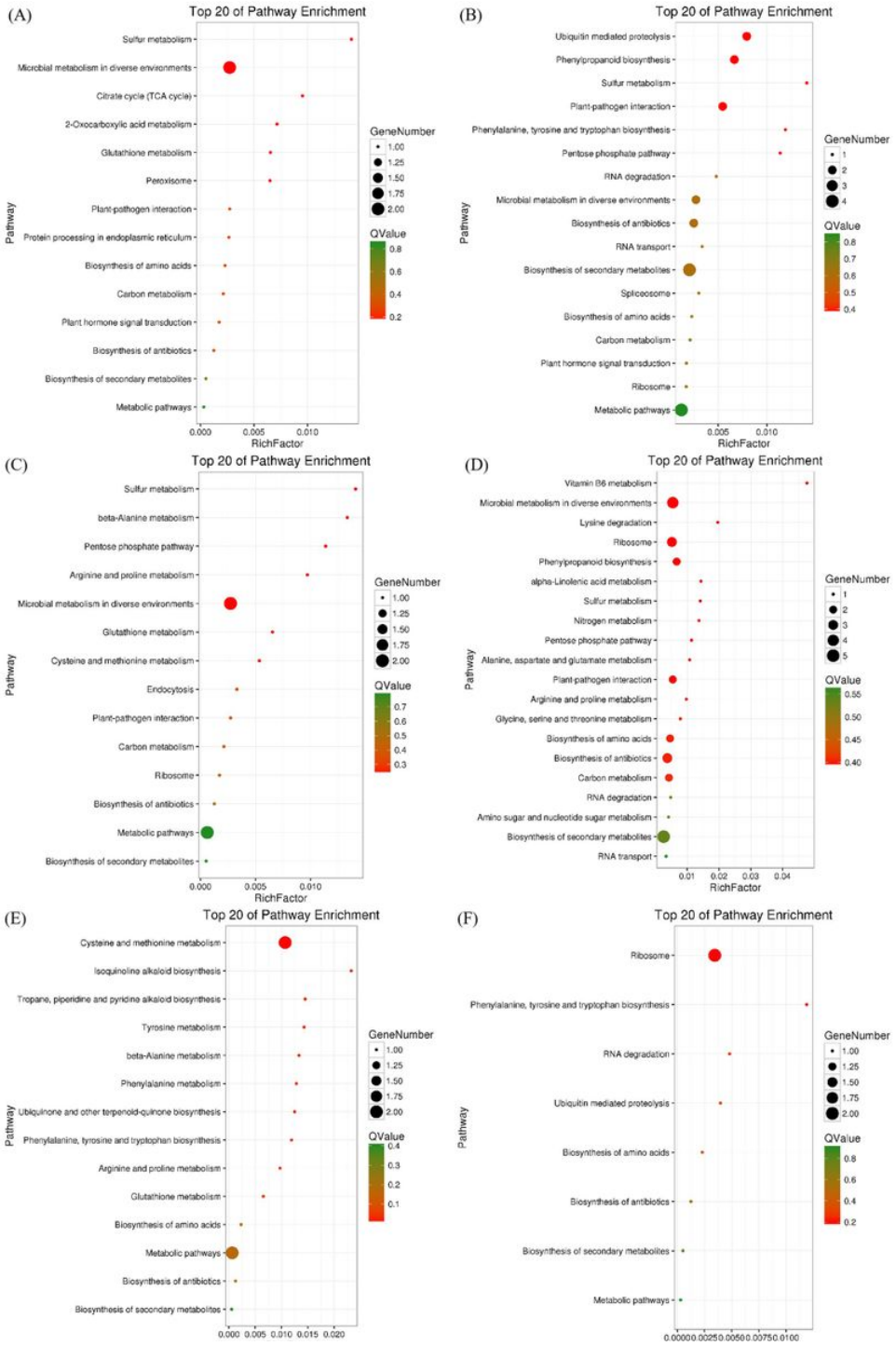

Figure 6

KEGG pathway enrichment analysis of the differentially expressed parental genes in response to P. brassicae infection at 8 and 23 dpi. KEGG pathways are listed on the left, whereas Q values and gene numbers are shown on the right. Top 20 enriched KEGG pathways in the control vs. Pb4 comparison at 8 dpi (A) and 23 dpi (B); and in the control vs. PbE comparison at 8 dpi (C) and 23 dpi (D); and the PbE vs. Pb4 comparison at 8 dpi (E) and 23 dpi (F).

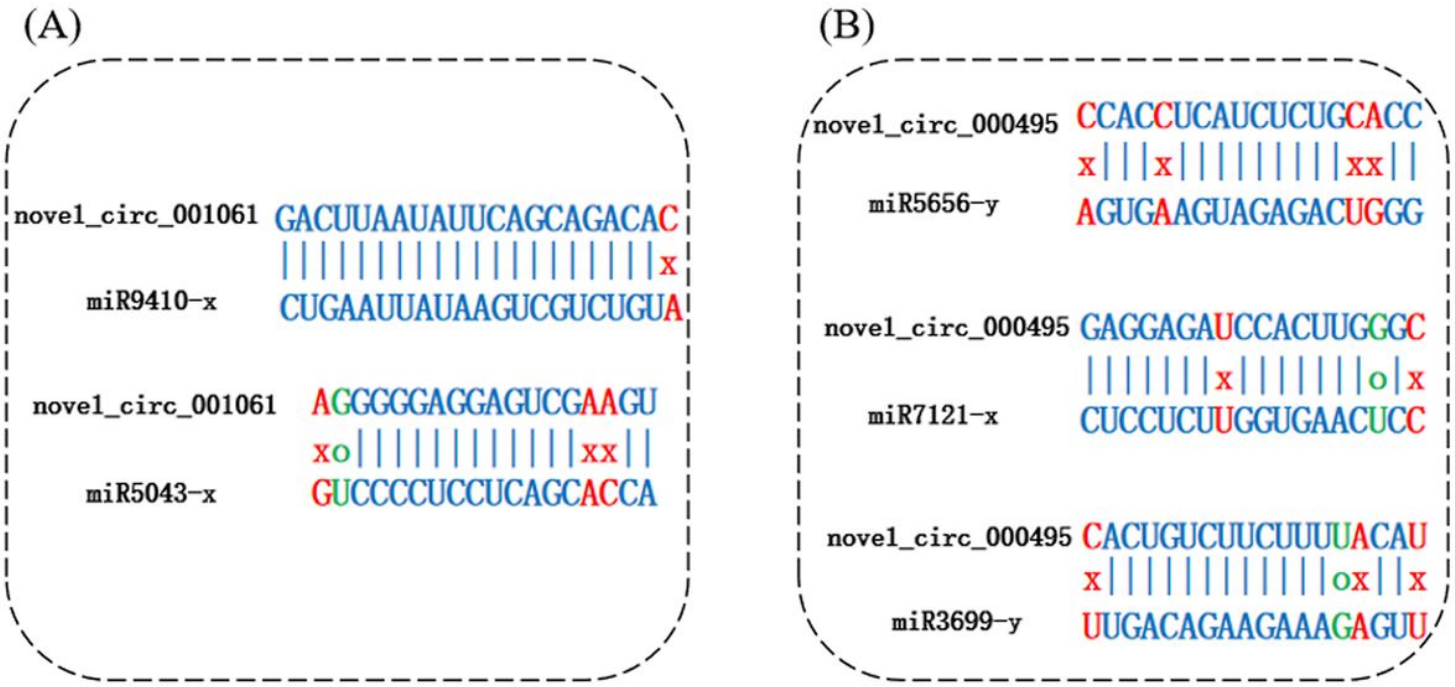

Figure 7

Potential interaction networks of miRNAs and circRNAs. Schema diagrams show the pairing of each circRNA sequence and the sequence of its target region.

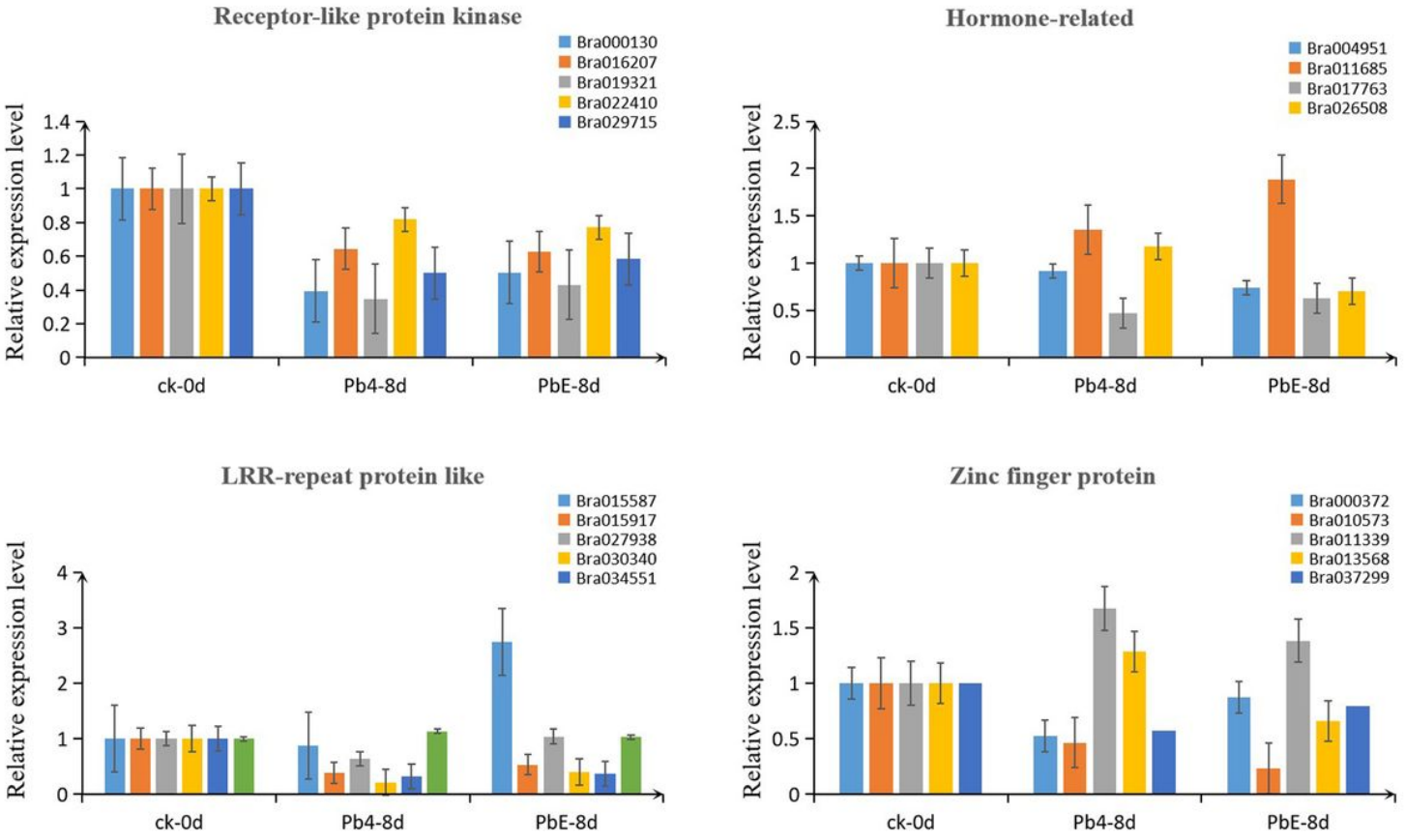

Figure 8

Expression of stress-associated genes at different stages.

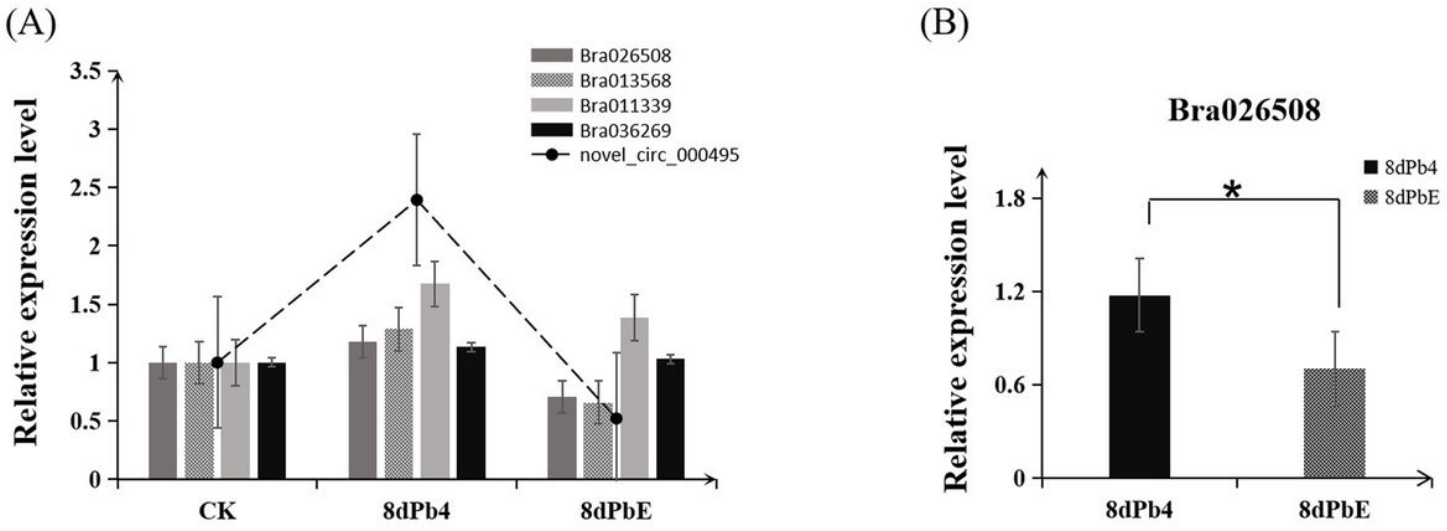

Figure 9

(A)The relative expression level of target genes and circRNAs in roots. (A)The relative expression of the Bra026508 in roots at 8dpi, respectively.*indicate that it is a significant difference at 0.05 level.

Supplementary Files

This is a list of supplementary files associated with this preprint. Click to download.

- Additionalfile1.jpg
- Additionalfile2.jpg
- Additionalfile3.jpg
- Additionalfile4.xlsx
- Additionalfile5.xlsx
- Additionalfile6.jpg
- Additionalfile7.xlsx
- Additionalfile8.xlsx
- Additionalfile9.xlsx
- Additionalfile10.jpg
- Additionalfile11.xlsx
- Additionalfile12.xlsx